Analysis of optical magnetoelectric effect in $GaFeO_3$

Jun-ichi Igarashi[1] and Tatsuya Nagao[2]
[1]*Faculty of Science, Ibaraki University, Mito, Ibaraki 310-8512, Japan*
[2]*Faculty of Engineering, Gunma University, Kiryu, Gunma 376-8515, Japan*
(Received 15 May 2009; published 31 August 2009)

We study the optical-absorption spectra in a polar ferrimagnet $GaFeO_3$. We consider the $E1$, $E2$, and $M1$ processes on Fe atoms. It is shown that the magnetoelectric effect on the absorption spectra arises from the $E1$-$M1$ interference process through the hybridization between the $4p$ and $3d$ states in the noncentrosymmetric environment of Fe atoms. We perform a microscopic calculation of the spectra on a cluster model of FeO_6 consisting of an octahedron of O atoms and an Fe atom displaced from the center with reasonable values for Coulomb interaction and hybridization. We obtain the magnetoelectric spectra, which depend on the direction of magnetization, as a function of photon energy in the optical region 1.0–2.5 eV, in agreement with the experiment.

DOI: 10.1103/PhysRevB.80.054418 PACS number(s): 78.20.Ls, 78.20.Bh, 78.40.−q

I. INTRODUCTION

It is known that the breaking of time-reversal symmetry in magnetic materials gives rise to interesting magneto-optical effects such as the double circular reflection for circularly polarized light and the Faraday effect for linearly polarized light.[1] When the spatial inversion symmetry is further broken, for example, in polar or chiral materials, novel magneto-optical effects were expected to come out.[2] Those effects are known as the nonreciprocal directional dichroism or magnetochiral dichroism and have been extensively studied.[3–7] Among a variety of compounds, Cr_2O_3 is one of the most investigated compounds. The magnetoelectric effect, that is, a linear relation between the magnetic and electric fields in matter was proved in 1950s.[8,9] Later, the nonreciprocal rotation and ellipticity of light were measured[10] and were successfully analyzed by using a ligand-field model for Cr atoms.[11]

Another notable compound is $GaFeO_3$, which was first synthesized by Remeika.[12] This compound exhibits simultaneously spontaneous electric polarization and magnetization at low temperatures. The large magnetoelectric effect was observed by Rado.[13] Recently, untwinned large single crystals have been prepared[14] and the optical-absorption measurement has been carried out with changing the direction of magnetization.[15] It has been found that the absorption intensity in the region of photon energy 1.0–2.5 eV changes with reversing the direction of the magnetization. The purpose of this paper is to analyze in detail this phenomenon by carrying out a microscopic calculation of the spectra and to elucidate the microscopic origin. Although several qualitative arguments have been done,[15,16] as far as we know, the spectra have not been calculated yet as a function of photon energy.

The crystal of $GaFeO_3$ has an orthorhombic unit cell with the space group $Pc2_1n$.[17] The magnetic moments at Fe1 and Fe2 sites align antiferromagnetically along the $\pm c$ axis. The actual compound, however, behaves as a ferrimagnet,[18] from which it is inferred that the Fe occupation at Fe1 and Fe2 sites are slightly different from each other.[14] Each Fe atom is octahedrally surrounded by O atoms and slightly displaced from the center of the octahedron; the shift is 0.26 Å at Fe1 sites and −0.11 Å at Fe2 sites along the b axis.[14] Thereby the spontaneous electric polarization is generated along the b axis. We neglect slight distortion of octahedrons since their contributions are expected to be small to the $E1$-$M1$ terms. There are two kinds of octahedrons with respect to the direction of Fe shift, as illustrated in Fig. 1.

In the analysis of optical absorption, we assume that the photon propagates along the a axis in accordance with the experimental situation.[15] Restricting the processes only on Fe atoms, we derive the explicit forms of $E1$, $E2$, and $M1$ transitions. We find that the $E2$ transition matrix elements are much smaller than those of the $E1$ and $M1$ transitions. In addition to the $E1$-$E1$ and $M1$-$M1$ processes, the $E1$-$M1$ interference process could have finite contribution to the optical absorption through the mixing of the $3d^4 4p$ configuration to the $3d^5$ configuration, as illustrated in Fig. 2. Such mixings are the result of the noncentrosymmetric environment on Fe atoms. In order to describe such processes, we employ a cluster model of FeO_6, which includes all the $3d$ and $4p$ orbitals of Fe atoms and the $2p$ orbitals of O atoms. The Coulomb interaction and the spin-orbit interaction are taken into account in the $3d$ orbitals. Since Fe atoms are located in the noncentrosymmetric environment, the $4p$ and $3d$ states could be coupled to each other. A similar cluster

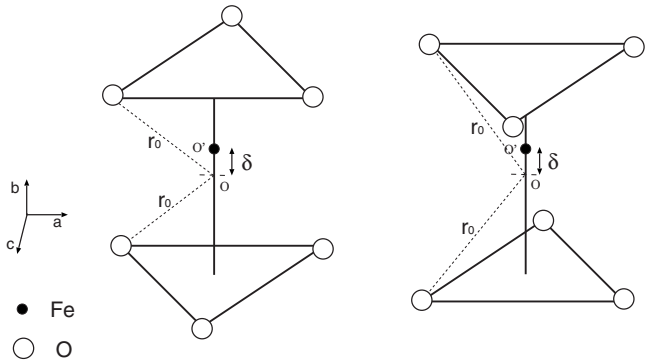

FIG. 1. Two kinds of octahedrons of oxygen atoms (white circles). Fe atoms (black circles) are displaced from the center of the octahedron O to the off-center O′ along the b axis by amount δ; δ=0.26 Å at Fe1 sites and δ=−0.11 Å at Fe2 sites.

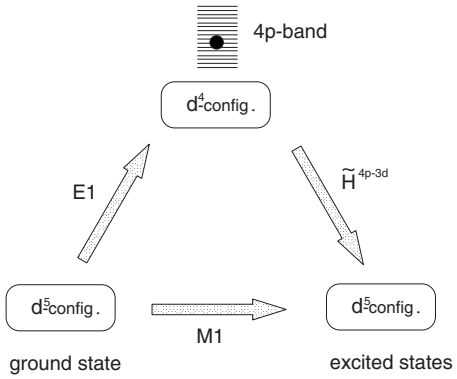

FIG. 2. Illustration of the $E1$-$M1$ interference process. The black circle indicates the presence of an electron in the $4p$ band.

model has been considered in the analysis of resonant x-ray scattering in magnetite,[19] where Fe atoms at A sites are in the noncentrosymmetric environment, at the center of tetrahedrons of O atoms. Deriving an effective hybridization between the $4p$ and $3d$ states as well as a ligand field on the $3d$ states through the hybridization with the O $2p$ states, we diagonalize the Hamiltonian matrix in the $3d^5$ and $3d^4$ configurations to obtain the energy eigenstates. These states are used to calculate the absorption spectra.

In the experiment, the magnetic field was applied along the $\pm c$ axis and the difference of the absorption spectra between the two directions was measured, which would be termed as "magnetoelectric" spectra.[15] Since the compound is a ferrimanget, reversing direction of applied magnetic field results in reversing the direction of the local magnetic moment on Fe atoms. Neglecting a small deviation from a perfect antiferromagnet, we simply assume that the direction of the local magnetic moment is simply reversed. We derive a formula for the magnetoelectric spectra which arise from the $E1$-$M1$ process. Using this formula, we discuss various symmetry relations for the $E1$-$M1$ process and the relation to the nonreciprocal directional dichroism and the anapole moment on these bases. Finally, we carry out a microscopic calculation of the spectra arising from the $E1$-$M1$ process using the results of the FeO_6 cluster model. We find the spectra as a function of photon energy in agreement with the experiment.[15]

This paper is organized as follows. In Sec. II, we introduce a cluster model around Fe atoms. In Sec. III, we describe the optical transition operators associated with Fe atoms. In Sec. IV, we derive the formulas of the optical absorption and present the calculated spectra in comparison with the experiment. The last section is devoted to concluding remarks.

II. ELECTRONIC STRUCTURES AROUND Fe ATOMS

A. Crystal electric field

We start by examining the crystal electric field around the off-center position $O'=(0,0,\delta)$ to see the effect of lowering symmetry from the cubic to trigonal ones. Let charge q be placed at the apexes of the octahedron. Then, the electrostatic potential $\phi(x,y,z)$ is expanded as

$$\phi(x,y,z) = V_0 + \delta V_1 + \delta^2 V_2 + \cdots, \tag{2.1}$$

with

$$V_0 = \frac{6q}{r_0} - \frac{7q}{24r_0^5}\{35z^4 - 30z^2r^2 + 3r^4 \pm 20\sqrt{2}z(x^3 - 3xy^2)\}, \tag{2.2}$$

$$V_1 = -\frac{14q}{3r_0^5}\left\{5z^3 - 3zr^2 \pm \frac{5}{4}\sqrt{2}(x^3 - 3xy^2)\right\}, \tag{2.3}$$

$$V_2 = -\frac{7q}{r_0^5}\{2z^2 - (x^2 + y^2)\}, \tag{2.4}$$

where the x, y, and z axes are along the crystal c, a, and b axes, respectively, with the origin O′. The distance between the center of the octahedron and the apexes is defined as r_0 and $r=\sqrt{x^2+y^2+z^2}$. The upper and lower signs correspond to the octahedron on the left and right panels in Fig. 1, respectively. Term V_0 represents the so-called cubic-field term, which gives rise to a splitting of energy between e_g and t_{2g} states in $3d$ orbitals. Term V_1 gives rise to a coupling between $3d$ and $4p$ states, and V_2 gives rise to additional splittings of energy within the $3d$ states as well as the $4p$ states. These forms are inferred to be correct in symmetry point of view but the covalency between Fe and O is, however, expected to give rise to a similar but much larger effect. We neglect the small point-charge effect and consider only the covalency effect discussed in the following.

B. Hamiltonian for a FeO_6 cluster

We now introduce the Hamiltonian of a FeO_6 cluster and derive the ligand field on the $3d$ states and the effective hybridization between the $3d$ and $4p$ states. With the $2p$ states in O atoms in addition to the $3d$ and $4p$ states in the Fe atom, we write the Hamiltonian as

$$H = H^{3d} + H^{2p} + H_{\rm hyb}^{3d-2p} + H^{4p} + H_{\rm hyb}^{4p-2p}, \tag{2.5}$$

where

$$H^{3d} = \sum_{m\sigma} E_m^d d_{m\sigma}^\dagger d_{m\sigma} + \frac{1}{2}\sum_{\nu_1\nu_2\nu_3\nu_4} g(\nu_1\nu_2;\nu_3\nu_4) d_{\nu_1}^\dagger d_{\nu_2}^\dagger d_{\nu_4} d_{\nu_3} + \zeta_{3d}\sum_{mm'\sigma\sigma'} \langle m\sigma|\mathbf{L}\cdot\mathbf{S}|m'\sigma'\rangle d_{m\sigma}^\dagger d_{m'\sigma'} + \mathbf{H}_{xc}\cdot\sum_{m\sigma\sigma'} (\mathbf{S})_{\sigma\sigma'} d_{m\sigma}^\dagger d_{m\sigma'}, \tag{2.6}$$

$$H^{2p} = \sum_{j\eta\sigma} E^p p_{j\eta\sigma}^\dagger p_{j\eta\sigma}, \tag{2.7}$$

$$H_{\rm hyb}^{3d-2p} = \sum_{j\eta\sigma m} t_{m\eta}^{3d-2p}(j) d_{m\sigma}^\dagger p_{j\eta\sigma} + \text{H.c.}, \tag{2.8}$$

$$H^{4p} = \sum_{\mathbf{k}\eta'\sigma} \epsilon_{4p}(\mathbf{k}) p_{\mathbf{k}\eta'\sigma}'^\dagger p_{\mathbf{k}\eta'\sigma}', \tag{2.9}$$

$$H_{\rm hyb}^{4p-2p} = \sum_{j\eta\sigma\eta'} t_{\eta'\eta}^{4p-2p}(j) p'^{\dagger}_{\eta'\sigma} p_{j\eta\sigma} + \text{H.c.} \qquad (2.10)$$

The H^{3d} describes the energy of $3d$ electrons, where $d_{m\sigma}$ represents an annihilation operator of a $3d$ electron with spin σ and orbital m $(=x^2-y^2, 3z^2-r^2, yz, zx, xy)$. The second term in Eq. (2.6) represents the intra-atomic Coulomb interaction with the matrix element $g(\nu_1\nu_2;\nu_3\nu_4)$ expressed in terms of the Slater integrals F^0, F^2, and F^4 [ν stands for (m,σ)]. The third term in Eq. (2.6) represents the spin-orbit interaction for $3d$ electrons. We evaluate atomic values of F^2, F^4, and ζ_{3d} within the Hartree-Fock (HF) approximation[20] and multiply 0.8 to these atomic values in order to take account of the slight screening effect. On the other hand, we multiply 0.25 to the atomic value for F^0 since F^0 is known to be considerably screened by solid-state effects. The last term in Eq. (2.6) describes the energy arising from the exchange interaction with neighboring Fe atoms, where $(\mathbf{S})_{\sigma\sigma'}$ represents the matrix element of the spin operator of $3d$ electrons. The exchange field $\mathbf{H}_{xc}$ here has a dimension of energy and is $\sim k_{\rm B}T_c/4$ with $T_c \sim 250$ K. Note that this term is served as selecting the ground state by lifting the degeneracy and therefore the spectra depend little on its absolute value. The $\mathbf{H}_{xc}$ is directed to the negative direction of the c axis at Fe1 sites when the external magnetic field is applied along the positive direction of the c axis.

The H^{2p} represents the energy of oxygen $2p$ electrons, where $p_{j\eta\sigma}$ is the annihilation operator of the $2p$ state with $\eta=x,y,z$ and spin σ at the oxygen site j. The Coulomb interaction is neglected in oxygen $2p$ states. The $H_{\rm hyb}^{3d-2p}$ denotes the hybridization energy between the $3d$ and $2p$ states. The energy of the $2p$ level relative to the $3d$ levels is determined from the charge-transfer energy Δ defined by $\Delta = E^d - E^p + 15U(3d^6) - 10U(3d^5)$ with E^d being an average of E_m^d. Here $U(3d^6)$ and $U(3d^5)$ are the multiplet-averaged d-d Coulomb interaction in the $3d^6$ and $3d^5$ configurations, which are defined by $U = F^0 - (2/63)F^2 - (2/63)F^4$.

The H^{4p} represents the energy of the $4p$ states, where $p'_{\mathbf{k}\eta'\sigma}$ is the annihilation operator of the $4p$ state with momentum $\mathbf{k}$, $\eta'=x,y,z$, and spin σ. The $4p$ states form an energy band $\epsilon_{4p}(\mathbf{k})$. The density of states (DOS) of the $4p$ band is inferred from the K-edge absorption spectra[21] as shown in Fig. 3. The $H_{\rm hyb}^{4p-2p}$ represents the hybridization between the $4p$ and oxygen $2p$ states, where the annihilation operator of the local $4p$ orbital $p'_{\eta'\sigma}$ may be expressed as $p'_{\eta'\sigma} = (1/\sqrt{N_0})\Sigma_{\mathbf{k}} p'_{\mathbf{k}\eta'\sigma}$ (N_0 is the discretized number of $\mathbf{k}$ points).

The hybridization matrices $t_{m\eta}^{3d-2p}(j)$ and $t_{\eta'\eta}^{4p-2p}(j)$ are defined for the Fe atom at the off-center position. We evaluate these values by modifying the Slater-Koster two-center integrals for the Fe atom at the central position of the octahedron with the assumption that $(pd\sigma)_{2p,3d}$, $(pd\pi)_{2p,3d} \propto d^{-4}$, and $(pp\sigma)_{4p,2p}$, $(pp\pi)_{4p,2p} \propto d^{-2}$ for d being the Fe-O distance.[22] Table I lists the parameter values used in this paper, which are consistent with the values in previous calculations for Fe_3O_4.[19,23]

C. Ligand field and effective hybridization between 4*p* and 3*d* states

Instead of directly treating H^{3d-2p} and H^{4p-2p}, we introduce the effective Hamiltonian to include the covalency effect. The ligand-field Hamiltonian on the $3d$ states is given by the second-order perturbation as

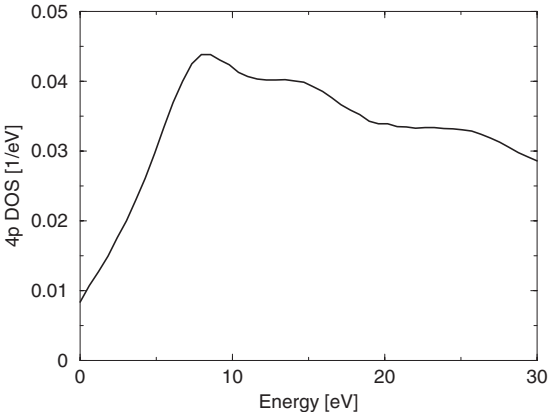

FIG. 3. Density of states of the $4p$ band. It is constructed from the experimental K-edge absorption spectra (Ref. 21) with cutting off the low-energy tail coming from the lifetime width of the core hole. The high-energy side is arbitrarily cutoff. The integrated value is normalized to unity.

$$\tilde{H}^{3d-3d} = \sum_{mm'\sigma} \tilde{t}_{mm'}^{3d-3d} d_{m\sigma}^{\dagger} d_{m'\sigma} + \text{H.c.}, \qquad (2.11)$$

with

$$\tilde{t}_{mm'}^{3d-3d} = \sum_{j\eta} t_{m\eta}^{3d-2p}(j) t_{m'\eta}^{3d-2p}(j)/\Delta, \qquad (2.12)$$

where the sum over j is taken on neighboring O sites and $\Delta = 3.3$ eV is the charge-transfer energy defined above. In addition to the ligand field corresponding to the cubic symmetry, we have a field proportional to δ^2, which causes extra splittings of $3d$ levels in conformity with the form of Eq. (2.1).

The effective hybridization between the $4p$ and $3d$ states is similarly given as

$$\tilde{H}^{4p-3d} = \sum_{\eta' m\sigma} \tilde{t}_{\eta' m}^{4p-3d} p'^{\dagger}_{\eta'\sigma} d_{m\sigma} + \text{H.c.}, \qquad (2.13)$$

with

$$\tilde{t}_{\eta' m}^{4p-3d} = \sum_{j\eta} t_{\eta'\eta}^{4p-2p}(j) t_{m\eta}^{3d-2p}(j)/(E^{4p} - E^{2p}), \qquad (2.14)$$

where E^{4p} is the average of the $4p$-band energy, which is estimated as $E^{4p} - E^{2p} \approx 17$ eV. The coefficient $\tilde{t}_{\eta' m}^{4p-3d}$ is

TABLE I. Parameter values for a FeO_6 cluster in the $3d^5$ configuration, in units of eV. The Slater-Koster two-center integrals are defined for the Fe atom at the center of the octahedron.

$F^0(3d,3d)$	6.39	$(pd\sigma)_{2p,3d}$	−1.9
$F^2(3d,3d)$	9.64	$(pd\pi)_{2p,3d}$	0.82
$F^4(3d,3d)$	6.03	$(pp\sigma)_{2p,4p}$	3.5
ζ_{3d}	0.059	$(pp\pi)_{2p,4p}$	−1.0
Δ	3.3		

nearly proportional to the shift δ of the Fe atom from the center of the octahedron, again in conformity with the form of Eq. (2.1).

III. ABSORPTION PROCESS ON Fe

The interaction between the electromagnetic wave and electrons is described by

$$H_{\rm int} = -\frac{1}{c}\int \mathbf{j}(\mathbf{r})\cdot\mathbf{A}(\mathbf{r})d^3\mathbf{r}, \tag{3.1}$$

where $\mathbf{j}$ represents the current-density operator and the electromagnetic field $\mathbf{A}(\mathbf{r})$ for linear polarization is defined as

$$\mathbf{A}(\mathbf{r}) = \sum_{\mathbf{q}} \sqrt{\frac{2\pi\hbar c^2}{V\omega_{\mathbf{q}}}}\mathbf{e}c_{\mathbf{q}}e^{i\mathbf{q}\cdot\mathbf{r}} + \text{H.c.}, \tag{3.2}$$

with $c_{\mathbf{q}}$ and $\mathbf{e}$ being the annihilation operator of photon and the unit vector of polarization, respectively. We approximate this expression into a sum of the contributions from each Fe atom

$$H_{\rm int} = -\frac{1}{c}\sum_{\mathbf{q},i}\mathbf{j}(\mathbf{q},i)\cdot\mathbf{A}(\mathbf{q},i) + \text{H.c.}, \tag{3.3}$$

with

$$\mathbf{j}(\mathbf{q},i) = \sum_{nn'}[\int e^{i\mathbf{q}\cdot(\mathbf{r}-\mathbf{r}_i)}\mathbf{j}_{nn'}(\mathbf{r}-\mathbf{r}_i)d^3(\mathbf{r}-\mathbf{r}_i)]a_n^\dagger(i)a_{n'}(i), \tag{3.4}$$

$$\mathbf{A}(\mathbf{q},i) = \sqrt{\frac{2\pi\hbar c^2}{V\omega_{\mathbf{q}}}}\mathbf{e}c_{\mathbf{q}}e^{i\mathbf{q}\cdot\mathbf{r}_i}, \tag{3.5}$$

where the local current operator may be described by

$$\mathbf{j}_{nn'}(\mathbf{r}-\mathbf{r}_i) = \frac{ie\hbar}{2m}[(\nabla\phi_n^*)\phi_{n'} - \phi_n^*\nabla\phi_{n'}] - \frac{e^2}{mc}\mathbf{A}\phi_n^*\phi_{n'} + \frac{e\hbar}{mc}c\nabla\times[\phi_n^*\mathbf{S}\phi_{n'}]. \tag{3.6}$$

The integration in Eq. (3.4) is carried out around site i and $a_n(i)$ is the annihilation operator of electron with the local orbital with the wave function $\phi_n(\mathbf{r}-\mathbf{r}_i)$. The e and m are the charge and the mass of electron, and $\hbar\mathbf{S}$ is the spin operator of electron. The second term in Eq. (3.6), which describes the scattering of photon, will be neglected in the following discussion. The approximation made by taking account of the process only on Fe atoms may be justified at the core-level spectra but less accurate in the optical region. The spectra arising from the magnetoelectric effect, however, are expected to be described rather well by the present approximation since such effects mainly take place on Fe atoms.

For later convenience, we write the interaction between the matter and the photon in a form,

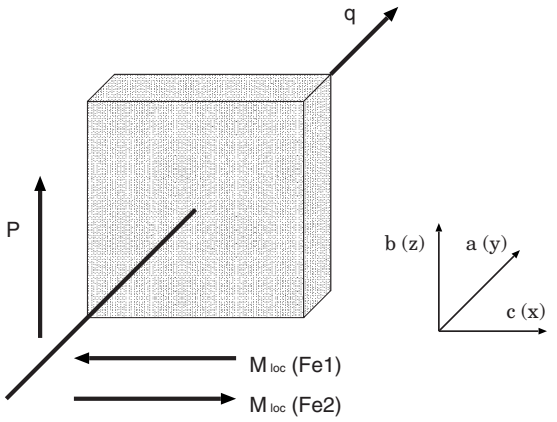

FIG. 4. Geometry of absorption. Light propagates along the a axis with polarization along the b axis or the c axis. The electric dipole moment is along the b axis. The sublattice magnetization is directed to the negative direction of the c axis at Fe1 sites and to the reverse at Fe2 sites, when the external magnetic field is applied to the positive direction of the c axis. When the external magnetic field is reversed, the sublattice magnetization is reversed.

$$H_{\rm int} = -e\sum_{\mathbf{q}}\sqrt{\frac{2\pi}{V\hbar\omega_{\mathbf{q}}}}\sum_i T(\mathbf{q},\mathbf{e},i)c_{\mathbf{q}}e^{i\mathbf{q}\cdot\mathbf{r}_i} + \text{H.c.} \tag{3.7}$$

To be specific in connection with the experimental setup,[15] we consider the situation that the photon propagates along the a axis with linear polarization, as illustrated in Fig. 4.

A. $E1$ transition

The transition operator $T(\mathbf{q},\mathbf{e},i)$ for the $E1$ transition is given by putting $e^{i\mathbf{q}\cdot(\mathbf{r}-\mathbf{r}_j)}=1$ in Eq. (3.4). Therefore it is independent of the propagation direction of photon. For the polarization along the z axis, the first term in Eq. (3.6) is rewritten by employing the following relation:

$$\int \phi_n^*\frac{\partial}{\partial z}\phi_{n'}d^3\mathbf{r} = -\frac{m}{\hbar^2}(\epsilon_n-\epsilon_{n'})\int\phi_n^* z\phi_{n'}d^3\mathbf{r}, \tag{3.8}$$

where ϵ_n and $\epsilon_{n'}$ are energy eigenvalues with ϕ_n and $\phi_{n'}$, respectively. The $4p$ and $3d$ states are assigned to ϕ_n and $\phi_{n'}$, respectively. Hence the transition operator T^{E1} is expressed as

$$T^{E1}(\mathbf{q},\mathbf{e},i) = iB^{E1}\sum_{i\eta m\sigma}N^{E1}_{\eta m}[p'^\dagger_{\eta\sigma}(i)d_{m\sigma}(i) - d^\dagger_{m\sigma}(i)p'_{\eta\sigma}(i)], \tag{3.9}$$

where i runs over Fe sites. The $N^{E1}_{\eta m}$'s are given by $N^{E1}_{x,zx}=1/\sqrt{5}$, $N^{E1}_{y,yz}=1/\sqrt{5}$, and $N^{E1}_{z,3z^2-r^2}=2/\sqrt{15}$ for the polarization along the z axis, $N^{E1}_{x,x^2-y^2}=1/\sqrt{5}$, $N^{E1}_{x,3z^2-r^2}=-1/\sqrt{15}$, $N^{E1}_{y,xy}=1/\sqrt{5}$, and $N^{E1}_{z,zx}=1/\sqrt{5}$ for the polarization along the x axis, and $N^{E1}_{x,xy}=1/\sqrt{5}$, $N^{E1}_{y,x^2-y^2}=-1/\sqrt{5}$, $N^{E1}_{y,3z^2-r^2}=1/\sqrt{15}$, and $N^{E1}_{z,yz}=1/\sqrt{5}$ for the polarization along the y axis, respectively. The coefficient B^{E1} is defined by

$$B^{E1} = (\epsilon_{4p} - \epsilon_{3d}) \int_0^\infty r^3 R_{4p}(r) R_{3d}(r) dr, \tag{3.10}$$

where $R_{3d}(r)$ and $R_{4p}(r)$ are radial wave functions of $3d$ and $4p$ states with energy ϵ_{3d} and ϵ_{4p} in the Fe atom. The energy difference $\epsilon_{4p}-\epsilon_{3d}$ is not directly related to the absorbed photon energy. Within the HF approximation in the $1s^2 3d^5 4p^{0.001}$ configuration of an Fe atom,[20] we estimate it as $B^{E1} \approx 7.7 \times 10^{-8}$ cm eV.

B. *E*2 transition

The transition operator for the $E2$ transition is given from the second term in the expansion $e^{i\mathbf{q}\cdot(\mathbf{r}-\mathbf{r}_i)} \approx 1 + i\mathbf{q}\cdot(\mathbf{r}-\mathbf{r}_i) + \cdots$ in Eq. (3.4). Let the photon be propagating along the y axis with the polarization parallel to the z axis. Then we could derive a relation,

$$\int \phi_n^* y \frac{\partial}{\partial z} \phi_{n'} d^3\mathbf{r} = -\frac{m}{\hbar^2}(\epsilon_n - \epsilon_{n'}) \int \phi_n^* \frac{yz}{2} \phi_{n'} d^3\mathbf{r} + \frac{i}{2} \int \phi_n^* L_x \phi_{n'} d^3\mathbf{r}, \tag{3.11}$$

where $\hbar L_x$ is the orbital angular momentum operator. The last term should be moved into the terms of the $M1$ transition. In the first term of Eq. (3.11), the relevant states for ϕ_n and $\phi_{n'}$ are both $3d$ states, and $\epsilon_n - \epsilon_{n'}$ may be an order of the ligand-field energy, which is less than 1 eV. Since $\langle r^2 \rangle$ is estimated within the HF approximation as[20]

$$\int_0^\infty r^4 R_{3d}^2(r) dr = 3.3 \times 10^{-17} \text{ cm}^2, \tag{3.12}$$

we notice that the contribution from the $E2$ transition is smaller than that from the $M1$ transition discussed in Sec. III C.

C. *M*1 transition

From the third term in Eq. (3.6), we have a relation

$$\int e^{i\mathbf{q}\cdot(\mathbf{r}-\mathbf{r}_i)} \nabla \times (\phi_n^* \mathbf{S} \phi_{n'}) d^3\mathbf{r} = -i\mathbf{q} \times \int \phi_n^* \mathbf{S} \phi_{n'} e^{i\mathbf{q}\cdot(\mathbf{r}-\mathbf{r}_i)} d^3\mathbf{r} \approx -i\mathbf{q} \times \int \phi_n^* \mathbf{S} \phi_{n'} d^3\mathbf{r}. \tag{3.13}$$

Adding the contribution of the last term of Eq. (3.11), we have a factor $\mathbf{L}+2\mathbf{S}$ in the transition operator. The $3d$ states are assigned to ϕ_n and $\phi_{n'}$. Hence the transition operator for the $M1$ transition is given by

$$T^{M1}(\mathbf{q},\mathbf{e},i) = i|\mathbf{q}|B^{M1} \sum_{imm'\sigma\sigma'} N^{M1}_{m\sigma,m'\sigma'} d^\dagger_{m\sigma}(i) d_{m'\sigma'}(i), \tag{3.14}$$

where $B^{M1} = \hbar^2/2m = 3.8 \times 10^{-16}$ cm^2 eV. For the photon propagating along the y axis with polarizations along the z and x axes, we have $N^{M1}_{m\sigma,m'\sigma'} = \langle m\sigma | L_x + 2S_x | m'\sigma' \rangle$ and $N^{M1}_{m\sigma,m'\sigma'} = \langle m\sigma | -(L_z + 2S_z) | m'\sigma' \rangle$, respectively.

IV. CALCULATION OF ABSORPTION SPECTRA

Restricting the processes only on Fe atoms, we sum up cross sections at Fe sites to obtain the absorption intensity $I(\omega_\mathbf{q}, \mathbf{e})$. Dividing it by the incident flux c/V, we have

$$I(\omega_\mathbf{q},\mathbf{e}) \propto \frac{4\pi^2 e^2}{\hbar^2 c} \frac{1}{\omega_\mathbf{q}} \sum_i \sum_f |\langle \Psi_f(i)| T(\mathbf{q},\mathbf{e},i) |\Psi_g(i)\rangle|^2 \delta(\hbar\omega_\mathbf{q} + E_g - E_f), \tag{4.1}$$

where $T(\mathbf{q},\mathbf{e},i) = T^{E1}(\mathbf{q},\mathbf{e},i) + T^{M1}(\mathbf{q},\mathbf{e},i)$, and $|\Psi_g(i)\rangle$ and $|\Psi_f(i)\rangle$ represent the ground and the final states with energy E_g and E_f at site i, respectively. The sum over f is taken over all the excited state at Fe sites.

We first calculate the energy eigenstates $|\Phi_n(d^5)\rangle$ with eigenenergy $E_n(d^5)$ in the $3d^5$ configuration, and $|\Phi_n(d^4)\rangle$ with eigenenergy $E_n(d^4)$ in the $3d^4$ configuration, by diagonalizing the Hamiltonian $H_{3d} + \tilde{H}^{3d-3d}$. As already stated in Sec. II, the exchange field $\mathbf{H}_{xc}$ in Eq. (2.6) is assumed to be directed to the negative direction of the $c(x)$ axis at Fe1 sites and the reverse direction at Fe2 sites when the external magnetic field is applied to the positive direction of the c axis. All the directions could be reversed by reversing the external magnetic field since the actual compound is a ferrimagnet. The shift δ of Fe atoms along the b axis is assumed $\delta = 0.26$ Å at Fe1 sites and $\delta = -0.11$ Å at Fe2 sites, respectively.

As regards the lowest-energy state $|\Phi_g(d^5)\rangle$, we have the state ${}^6A_1$ under the trigonal crystal field, if we disregard the exchange field and the spin-orbit interaction. The inclusion of these interactions could induce the orbital moment $\langle L_x \rangle$ but its absolute value is given less than 0.004. Two types of octahedrons give the same angular momentum.

Within the first-order perturbation with the effective hybridization $\tilde{H}^{4p-3d}$, we could express the ground state $|\Psi_g(i)\rangle$ and the optical final states $|\Psi_f(i)\rangle$ as

$$|\Psi_g(i)\rangle = |\Phi_g(d^5)\rangle + \sum_{n\mathbf{k}\eta\sigma} |\Phi_n(d^4), \mathbf{k}\eta\sigma\rangle \frac{1}{E_g(d^5) - [E_n(d^4) + \epsilon_{4p}(\mathbf{k})]} \times \langle \Phi_n(d^4), \mathbf{k}\eta\sigma | \tilde{H}^{4p-3d} | \Phi_g(d^5)\rangle, \tag{4.2}$$

$$|\Psi_f(i)\rangle = |\Phi_f(d^5)\rangle + \sum_{n\mathbf{k}\eta\sigma} |\Phi_n(d^4), \mathbf{k}\eta\sigma\rangle \frac{1}{E_f(d^5) - [E_n(d^4) + \epsilon_{4p}(\mathbf{k})]} \times \langle \Phi_n(d^4), \mathbf{k}\eta\sigma | \tilde{H}^{4p-3d} | \Phi_f(d^5)\rangle, \tag{4.3}$$

with $E_g = E_g(d^5)$ and $E_f = E_f(d^5)$ being the lowest and excited energies in the d^5 configurations, respectively. Here $|\Phi_n(d^4), \mathbf{k}\eta\sigma\rangle$ represents the state of four electrons in the $3d$ states and one electron on the $4p$ states specified by $\eta(=x,y,z)$, spin σ, and momentum $\mathbf{k}$. The sum over $\mathbf{k}$ may be replaced by the integral with the $4p$ DOS. The explicit dependence on site i is abbreviated in the right-hand side of Eqs. (4.2) and (4.3). From these wave functions we obtain the expressions of optical transition amplitudes at site i by

$$M^{E1}(\mathbf{q},\mathbf{e},i;f) \equiv \langle \Psi_f(i)|T^{E1}(\mathbf{q},\mathbf{e},i)|\Psi_g(i)\rangle = \sum_{n\mathbf{k}\eta\sigma} \langle \Phi_f(d^5)|T^{E1}(\mathbf{q},\mathbf{e},i)|\Phi_n(d^4),\mathbf{k}\eta\sigma\rangle$$
$$\times \frac{1}{E_g(d^5) - E_n(d^4) - \epsilon_{4p}(\mathbf{k})} \langle \Phi_n(d^4),\mathbf{k}\eta\sigma|\tilde{H}^{4p-3d}|\Phi_g(d^5)\rangle + \sum_{n\mathbf{k}\eta\sigma} \langle \Phi_f(d^5)|\tilde{H}^{4p-3d}|\Phi_n(d^4),\mathbf{k}\eta\sigma\rangle$$
$$\times \frac{1}{E_f(d^5) - E_n(d^4) - \epsilon_{4p}(\mathbf{k})} \langle \Phi_n(d^4),\mathbf{k}\eta\sigma|T^{E1}(\mathbf{q},\mathbf{e},i)|\Phi_g(d^5)\rangle, \tag{4.4}$$

$$M^{M1}(\mathbf{q},\mathbf{e},i;f) \equiv \langle \Psi_f(i)|T^{M1}(\mathbf{q},\mathbf{e},i)|\Psi_g(i)\rangle$$
$$= \langle \Phi_f(d^5)|T^{M1}(\mathbf{q},\mathbf{e},i)|\Phi_g(d^5)\rangle. \tag{4.5}$$

With these amplitudes, we have

$$I(\omega_\mathbf{q},\mathbf{e}) \propto \frac{1}{\hbar\omega_\mathbf{q}} \sum_i \sum_f |M^{E1}(\mathbf{q},\mathbf{e},i;f) + M^{M1}(\mathbf{q},\mathbf{e},i;f)|^2 \delta[\hbar\omega_\mathbf{q} + E_g(d^5) - E_f(d^5)]. \tag{4.6}$$

Now we examine the symmetry relation of the amplitudes. First, let the propagating direction of photon be reversed with keeping other conditions. The magnetic field associated with the photon is reversed, N^{M1}'s in Eq. (3.14) change their signs. Since other conditions are the same, we have the new amplitudes $(M^{E1})' = M^{E1}$ and $(M^{M1})' = -M^{M1}$. Second, let the local magnetic moment at each Fe atom be reversed with keeping the same shifts from the center of octahedron. The reversing of the local magnetic moment corresponds to taking the complex conjugate of wave functions. Considering Eq. (4.4) together with Eq. (3.9), we have $(M^{E1})' = -(M^{E1})^*$. Also, considering Eq. (4.5) together with Eq. (3.14), we have $(M^{M1})' = (M^{M1})^*$. Third, let the shifts of Fe atoms from the center of octahedron be reversed with keeping the same local magnetic moment, which means the reversal of the direction of the local *electric* dipole moment. This operation gives rise to reversing the sign of $\tilde{H}^{4p-3d}$ but no change in the $3d$ states with the $3d^5$ and $3d^4$ configurations because the ligand field $\tilde{H}^{3d-3d}$ changes according to δ^2. As a result, we have the new amplitude $(M^{E1})' = -M^{E1}$ from Eq. (3.9) but no change $(M^{M1})' = M^{M1}$.

As already stated, the direction of the local magnetic moment could be reversed by reversing the direction of the applied magnetic field since the actual material is a ferrimagnet with slightly deviating from a perfect antiferromagnet. We define $\Delta I(\omega_\mathbf{q},\mathbf{e})$ by the difference between the absorption intensity with the applied magnetic field along the positive direction of the c axis and that with the field along the reverse direction. From the second symmetry relation mentioned above, we have

$$\Delta I(\omega_\mathbf{q},\mathbf{e}) \propto \frac{2}{\hbar\omega_\mathbf{q}} \sum_i \sum_f \{[M^{E1}(\mathbf{q},\mathbf{e},i;f)]^* M^{M1}(\mathbf{q},\mathbf{e},i;f) + [M^{M1}(\mathbf{q},\mathbf{e},i;f)]^* M^{E1}(\mathbf{q},\mathbf{e},i;f)\} \delta[\hbar\omega_\mathbf{q} + E_g(d^5) - E_f(d^5)]. \tag{4.7}$$

Considering the sign change, we infer from the above symmetry relations that

$$\Delta I(\omega_\mathbf{q},\mathbf{e}) \propto \frac{\mathbf{q}}{|\mathbf{q}|} \cdot \sum_i \mathbf{P}_{\rm loc}(i) \times \mathbf{M}_{\rm loc}(i), \tag{4.8}$$

where $\mathbf{P}_{\rm loc}(i)$ and $\mathbf{M}_{\rm loc}(i)$ are the electric and the magnetic dipole moment of Fe atom at site i, respectively [$\mathbf{P}_{\rm loc}(i) \propto \boldsymbol{\delta}_i \equiv (0,0,\delta)$]. This relation may be regarded as a lowest-order expansion with respect to $\boldsymbol{\delta}_i$ and $\mathbf{M}_{\rm loc}(i)$. The right-hand side of Eq. (4.8) is the sum of the local toroidal moment $\boldsymbol{\tau}(i)$ [$\equiv \boldsymbol{\delta}_i \times \mathbf{M}_{\rm loc}(i)$].[24]

Figure 5 shows the calculated $\Delta I(\omega_\mathbf{q},\mathbf{e})$ as a function of $\omega_\mathbf{q}$, in comparison with the experiment. We have replaced the δ function $\delta(x)$ in Eq. (4.7) by a Lorentzian form $(\gamma/\pi)/(x^2+\gamma^2)$ with $\gamma = 0.1$ eV. The calculated peak height at ~ 1.2 eV is set to be the same as the experimental one for the polarization $\mathbf{e}$ along the b axis. We have a two-peak structure around $\hbar\omega_\mathbf{q} = 1.0-1.5$ eV in agreement with the experiment but could not reproduce a dip found experimentally around $\hbar\omega_\mathbf{q} = 1.7-2.3$ eV. On the other hand, without further adjustment, we have a considerable dip around $\hbar\omega_\mathbf{q} = 2.0-2.5$ eV for $\mathbf{e}$ along the c axis, in agreement with the experiments.

Fe atoms are under the cubic symmetry without displacement, and the lowest and low-lying excited states are char-

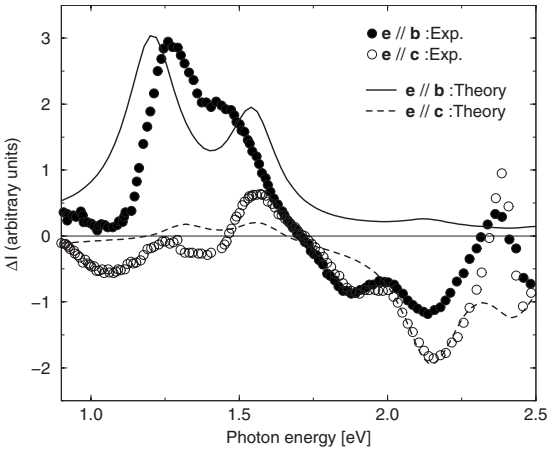

FIG. 5. Difference of absorption intensities $\Delta I(\omega_\mathbf{q},\mathbf{e})$ as a function of photon energy $\hbar\omega_\mathbf{q}$ between the applied magnetic field along the positive and negative directions of the c axis. Photon propagates along the positive a axis with polarization vector $\mathbf{e}$ along the b and c axes, respectively. Experimental data are taken from Ref. 15.

acterized as $^6A_1$, $^2T_2$, $^4T_1$, and $^4T_2$ with neglecting the spin-orbit interaction and the exchange field.[25] The excitation energies for $^2T_2$, $^4T_1$, and $^4T_2$ are estimated 1.34, 1.59, and 2.45 eV, respectively, within the present cluster model. Note that the direct absorption processes $^6A_1 \rightarrow {}^2T_2$, $^6A_1 \rightarrow {}^4T_1$, and $^6A_1 \rightarrow {}^4T_2$ are forbidden. The displacement of the Fe atom generates a trigonal field and makes the energy levels of the excited states split. The spin-orbit interaction and the exchange field further modify these states. The magnetoelectric spectra around 1.0–1.5 eV and around 1.7–2.3 eV might be interpreted as transitions to the states dispersed from $^2T_2$ and $^4T_1$, and those from $^4T_2$, respectively.

V. CONCLUDING REMARKS

We have studied the magnetoelectric effects on the optical-absorption spectra in a polar ferrimagnet $GaFeO_3$. We have considered the $E1$, $E2$, and $M1$ processes on Fe atoms, and have performed a microscopic calculation of the magnetoelectric spectra using a cluster model of FeO_6. The cluster consists of an octahedron of O atoms and an Fe atom displaced from the center of octahedron. We have disregarded additional small distortions of the octrahedron. Due to the noncentrosymmetric environment on the Fe atom, we have an effective hybridization between the $4p$ and $3d$ states through the O $2p$ states and thereby the mixing of the $3d^4 4p$ configuration to the $3d^5$ configuration. This mixing makes the $E1$-$M1$ interference process survive and gives rise to the magnetoelectric spectra. We have evaluated the $E1$-$M1$ process by using the energy eigenstates given in the $3d^4 4p$ configuration and the $3d^5$ configuration. The Coulomb interaction between $3d$ electrons and the hybridization are assumed to be nearly the same as previous cluster calculations.[19,23] We have obtained the magnetoelectric spectra as a function of photon energy in the optical region 1.0–2.5 eV, in agreement with the experiment.

In the experiment, the conventional absorption spectra, a part independent of the direction of magnetization, were measured with intensity about three orders of magnitude larger than the magnetoelectric part.[15] On the other hand, in the present approach considering only the local process on Fe atoms, the "total" intensity, which is given by the $E1$-$E1$ and $M1$-$M1$ processes, is estimated as merely one order-of-magnitude larger than that of the $E1$-$M1$ process. This suggests that other processes such as the transition from the valence band to the conduction band involving Ga and O atoms may add larger contributions. As far as the magnetoelectric spectra are concerned, however, the present approach considering only the local process on Fe atoms is expected to work well since the $E1$-$M1$ interference process could take place only on Fe atoms. Finally, from a different point of view, we would like to comment that the approach of considering the multiple scattering of a $4p$ electron in the noncentrosymmetric potential and the Coulomb interaction between the $4pd^4$ and the d^5 configurations may improve the above situation. The critical study is left in future.

We have concentrated on the spectra in the optical region. In the x-ray region, the magnetoelectric effects have also been studied.[21,26–29] Since the core electron is excited there, the local approach in this paper would be better applicable to the x-ray region than to the optical region, where the $E1$-$E2$ (not $E1$-$M1$) interference process gives rise to the magnetoelectric spectra. It may be interesting to analyze microscopically the nonreciprocal directional dichroism observed in the Fe pre-K-edge x-ray absorption in $GaFeO_3$ (Ref. 21) by using a similar cluster model. In this context, we would like to comment that the magnetoelectric effect on the resonant x-ray scattering spectra has been analyzed at the Fe pre-K-edge in Fe_3O_4,[19] where Fe atoms at A sites are located at the center of tetrahedron in noncentrosymmetric environment.

ACKNOWLEDGMENT

This work was partly supported by Grant-in-Aid for Scientific Research from the Ministry of Education, Culture, Sport, Science, and Technology, Japan.

[1] L. D. Landau, E. M. Lifshitz, and L. P. Pitaevskii, *Electrodynamics of Continuous Media* (Pergamon, Oxford, 1984).
[2] See, for example, R. M. Hornreich and S. Shtrikman, Phys. Rev. **171**, 1065 (1968); R. V. Pisarev, Zh. Eksp. Teor. Fiz. **58**, 1421 (1970) [Sov. Phys. JETP **31**, 761 (1970)].
[3] V. A. Markelov, M. A. Novikov, and A. A. Turkin, Zh. Eksp. Teor. Fiz. **25**, 404 (1977) [JETP Lett. **25**, 378 (1977)].
[4] E. L. Bubis and M. A. Novikov, Zh. Tekh. Fiz. **52**, 399 (1982) [Sov. Phys. Tech. Phys. **27**, 257 (1982)].
[5] G. L. J. A. Rikken and E. Raupach, Nature (London) **390**, 493 (1997).
[6] P. Kleindienst and G. H. Wagnière, Chem. Phys. Lett. **288**, 89 (1998).
[7] G. L. J. A. Rikken, C. Strohm, and P. Wyder, Phys. Rev. Lett. **89**, 133005 (2002).
[8] I. E. Dzyaloshinskii, Zh. Eksp. Teor. Fiz. **37**, 881 (1959) [Sov. Phys. JETP **10**, 628 (1960)].
[9] D. N. Astrov, Zh. Eksp. Teor. Fiz. **38**, 984 (1960) [Sov. Phys. JETP **11**, 708 (1960)].
[10] B. B. Krichevtsov, V. V. Pavlov, R. V. Pisarev, and V. N. Gridnev, Phys. Rev. Lett. **76**, 4628 (1996).
[11] M. Muto, Y. Tanabe, T. Iizuka-Sakano, and E. Hanamura, Phys. Rev. B **57**, 9586 (1998).
[12] J. P. Remeika, J. Appl. Phys. **31**, S263 (1960).
[13] G. T. Rado, Phys. Rev. Lett. **13**, 335 (1964).
[14] T. Arima, D. Higashiyama, Y. Kaneko, J. P. He, T. Goto, S. Miyasaka, T. Kimura, K. Oikawa, T. Kamiyama, R. Kumai, and Y. Tokura, Phys. Rev. B **70**, 064426 (2004).
[15] J. H. Jung, M. Matsubara, T. Arima, J. P. He, Y. Kaneko, and Y. Tokura, Phys. Rev. Lett. **93**, 037403 (2004).
[16] Y. Ogawa, Y. Kaneko, J. P. He, X. Z. Yu, T. Arima, and Y. Tokura, Phys. Rev. Lett. **92**, 047401 (2004).

[17] E. A. Wood, Acta Crystallogr. **13**, 682 (1960).
[18] R. B. Frankel, N. A. Blum, S. Foner, A. J. Freeman, and M. Schieber, Phys. Rev. Lett. **15**, 958 (1965).
[19] J. Igarashi and T. Nagao, J. Phys. Soc. Jpn. **77**, 084706 (2008).
[20] R. Cowan, *The Theory of Atomic Structure and Spectra* (University of California, Berkeley, 1981).
[21] M. Kubota, T. Arima, Y. Kaneko, J. P. He, X. Z. Yu, and Y. Tokura, Phys. Rev. Lett. **92**, 137401 (2004).
[22] W. A. Harrison, *Elementary Electronic Structure* (World Scientific, Singapore, 2004).
[23] J. Chen, D. J. Huang, A. Tanaka, C. F. Chang, S. C. Chung, W. B. Wu, and C. T. Chen, Phys. Rev. B **69**, 085107 (2004).
[24] Y. F. Popov, A. M. Kadomtseva, G. P. Vorob'ev, V. A. Timofeeva, D. M. Ustinin, A. K. Zvezdin, and M. M. Tegeranchi, Zh. Eksp. Teor. Fiz. **114**, 263 (1998) [Sov. Phys. JETP **87**, 146 (1998)].
[25] Y. Tanabe and S. Sugano, J. Phys. Soc. Jpn. **9**, 766 (1954).
[26] J. Goulon, A. Rogalev, F. Wilhelm, C. Goulon-Ginet, P. Carra, D. Cabaret, and C. Brouder, Phys. Rev. Lett. **88**, 237401 (2002).
[27] S. DiMatteo and C. R. Natoli, Phys. Rev. B **66**, 212413 (2002).
[28] P. Carra, A. Jerez, and I. Marri, Phys. Rev. B **67**, 045111 (2003).
[29] S. W. Lovesey, K. S. Knight, and E. Balcar, J. Phys.: Condens. Matter **19**, 376205 (2007).